

Flexible Arrays of Ni/Polyimide/Cu Microplasma Devices with a Dielectric Barrier and Excimer Laser Ablated Microcavities

S.-J. PARK, J. G. EDEN*, K. JAIN^{1†} and M. A. KLOSNER^{1‡}

Laboratory for Optical Physics and Engineering, Department of Electrical and Computer Engineering, University of Illinois, 1406 W. Green St., Urbana, IL 61801, U.S.A.

¹Anvik Corporation, 6 Skyline Dr., Hawthorne, NY 10532, U.S.A.

(Received February 2, 2006; accepted June 30, 2006; published online October 24, 2006)

Microcavity plasma devices with circular, crescent or, for example, trapezoidal cross-section microcavities (characteristic dimension $d = 30\text{--}100\ \mu\text{m}$), produced by excimer laser ablation and overcoated with a silicon nitride barrier film, have been fabricated in Ni/30 μm polyimide/3 μm Cu layered substrates. 12×12 arrays of devices with cylindrical microcavities 100 μm in diameter exhibit turn-on voltages of 255–270 V_{rms} for a Ne pressure of 700 Torr and a sinusoidal excitation voltage having a frequency of 5–20 kHz. All of the device designs explored to date operate in the abnormal glow region, and an increase of 15–20% in the ignition voltage for these arrays is observed when pd is raised from 4 to 5 Torr cm. Tests in which the arrays were *intentionally* damaged or photoablation parameters were altered from the optimal values show the microplasma devices to be extraordinarily robust and insensitive to the cross-sectional shape of the microcavity.

[DOI: 10.1143/JJAP.45.8221]

KEYWORDS: microplasma, photoablation, flexible arrays, microcavities

1. Introduction

Although the first plasma devices with a sub-mm cathode aperture were reported by White in 1959,¹⁾ a concerted effort to pursue the properties of plasmas confined to cavities with characteristic dimensions $<500\ \mu\text{m}$ began roughly a decade ago. In the intervening years, it has become evident that such microplasmas have properties attractive for applications as diverse as the destruction of volatile organic compounds^{2,3)} and the efficient generation of deep-ultraviolet (UV) or vacuum ultraviolet (VUV) radiation.⁴⁾ Details concerning these and other emerging applications of microplasma devices can be found in ref. 5.

Commercial adoption of microplasma technology will, to a significant degree, hinge on the development of device structures that are robust and yet are fabricated in inexpensive materials by processes amenable to large volume production methods such as roll-to-roll processing. However, it is customary in the literature of electronic and optical devices, in general, to report structures that have been optimized, leaving unanswered the question of potential degradations in performance arising from the variations in processing conditions that inevitably occur in manufacturing.

This paper presents the results of experiments characterizing a microplasma device structure that has proven to be exceptionally robust, despite processing conditions that are far from optimal. With a dielectric barrier and microcavities produced in thin polyimide layers on a Cu substrate by excimer laser photoablation, these devices can be fabricated on large sheets by roll-to-roll processing and yet are insensitive to the microcavity cross-section.

2. Device Structure and Fabrication Process

A cross-sectional diagram (not to scale) of the generalized microcavity plasma device structure adopted for these

experiments is illustrated in Fig. 1. The flexible and inexpensive substrate for these devices comprises 3–5 μm of Cu on $\sim 30\ \mu\text{m}$ of Kapton. After micromachining in the polyimide film the device cavity of the desired cross-sectional geometry by excimer laser (KrF) ablation, a 1.5 μm thick silicon nitride film was deposited within the cavity and onto the surrounding Kapton surface by plasma-enhanced chemical vapor deposition. Subsequently, a 0.1–0.15 μm thick Ni film was deposited around the perimeter of each microcavity by electron beam evaporation and, for a number of the microcavity plasma devices, a Ni screen electrode⁶⁾ of 600 mesh and 17 μm in thickness was also bonded to the device, as indicated in Fig. 1.

All of the microcavities were ablated with an Anvik Corp. photolithography system, of which a portion is shown schematically in Fig. 2. The deep ultraviolet ($\lambda = 248.4\ \text{nm}$) radiation from the excimer laser, which was operated at a pulse repetition frequency (PRF) of 200 Hz, was directed into an illumination system that both homogenizes the beam and alters its cross-section. Specifically, the rectangular cross-section of the beam produced by the laser is transformed into a hexagon-shaped radiation pattern with an intensity profile that is uniform to within 5%. After passing through the mask, the homogenized beam is imaged onto the substrate with a 1 : 1 projection lens. For an energy fluence at the polymer/Cu surface of 200–400 mJ cm^{-2} , ablating 30 μm of polyimide requires no more than 200 laser pulses and thus the laser dwell time per microcavity is typically 0.5–1 s. For most of the devices fabricated to date, the ablation process was terminated at the polyimide/Cu interface but, as suggested by Fig. 1, the microcavity for several devices extended a short distance (1–1.5 μm) into the Cu film. It should also be emphasized that a system closely related to that of Fig. 2 is the Anvik HexScan 3100 system which is designed for roll-to-roll processing. Consequently, although the experimental results reported here are associated with arrays fabricated on substrate areas as large as 100 cm^2 , the structure of Fig. 1 is designed to facilitate the transition to high speed production of microcavity plasma arrays in large flexible sheets.

*E-mail address: jgeden@uiuc.edu

[†]Present address: Department of Electrical and Computer Engineering, University of Illinois, 1406 W. Green St., Urbana, IL 61801, U.S.A.

[‡]Present address: Light Age, Inc., 500 Apgar Drive, Somerset, NJ 08873, U.S.A.

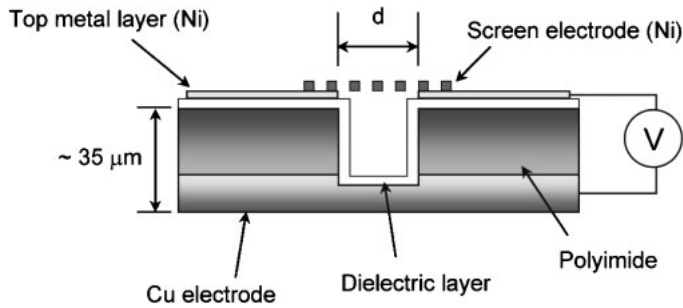


Fig. 1. Diagram (not to scale) of the microplasma device structure in cross-section. A number of single devices and large arrays were also fabricated without the screen electrode. The thicknesses of the silicon nitride and Ni films were 1.5 μm and 0.1–0.15 μm, respectively.

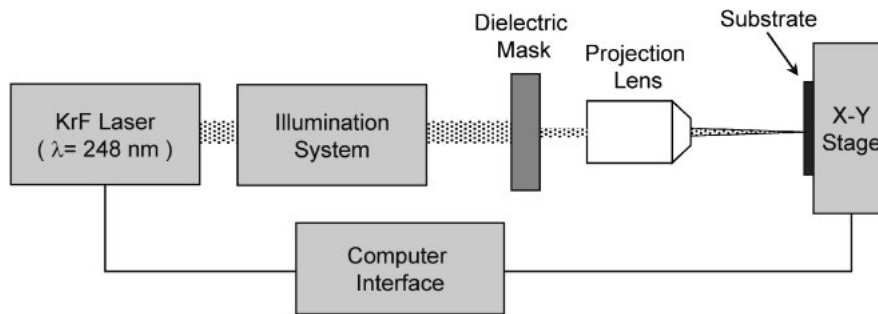


Fig. 2. Schematic diagram of the projection imaging, excimer laser photoablation system with which the microcavities were produced. Throughout these experiments, the laser wavelength was 248.4 nm (KrF).

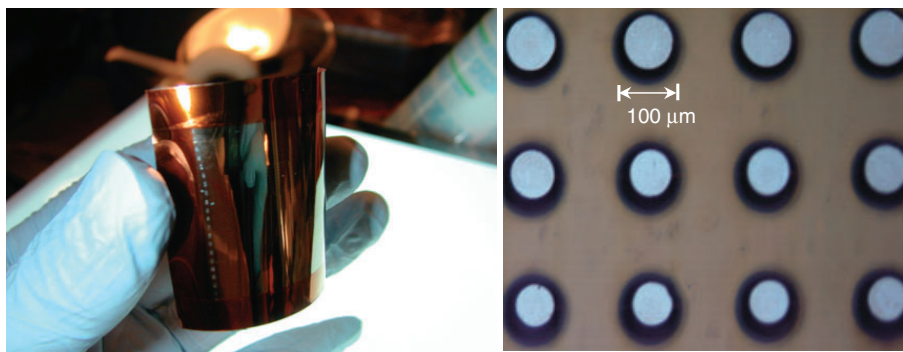


Fig. 3. Photographs of: (left) an array of microplasma devices, illustrating the flexibility of the structure; (right) 3 × 4 segment of Ni/silicon nitride/polyimide/Cu microcavity plasma devices that is a portion of a larger array. The cylindrical microcavities are 100 μm in dia. and the apparent asymmetry of several of the devices shown is an artifact of the microscope and the area size being imaged.

This system produces cavities of exceptional uniformity, and clean sidewalls. Figure 3 presents two photographs of completed arrays. At left, the flexibility of this thin array structure is evident. A 12 device segment (3 × 4) of a larger array of Ni/silicon nitride/polyimide/Cu devices with 100 μm dia. cavities is shown by the optical micrograph on the right side of Fig. 3.

Before leaving this section, it should be noted that the structure of Fig. 1 is similar to that of the DC-driven metal/polymer/metal devices first described by Park *et al.*⁷⁾ and subsequently applied by Sankaran and Giapis⁸⁾ to the etching of Si. As will be evident later, the incorporation of the dielectric barrier improves dramatically the ruggedness and lifetime of these devices.

3. Experimental Results and Discussion

3.1 Optical and electrical characteristics

An optical micrograph of four 6 × 6 arrays comprising devices having the structure of Fig. 1 is presented in Fig. 4. Shown operating in 500 Torr of Ne and driven by a 20 kHz

sinusoidal AC driving voltage, these devices were fabricated in a 30 μm polyimide/3 μm Cu substrate and the 100 μm dia. microcavities have a 200 μm pitch. Each microplasma device produces a diffuse glow but extension of the plasma over a portion of the surface of the array is evident between several of the devices in the subarrays. As one would expect, this effect vanishes at lower current levels and optimization of the microcavity aspect ratio (depth-to-diameter) and dielectric thickness is expected to confine the microplasmas within the cavities at higher current levels.

Figure 5 shows the voltage–current (*V–I*) characteristics for the array of Figs. 3 and 4. These data were acquired at a Ne pressure (*p*_{Ne}) of 700 Torr and sinusoidal driving voltage frequencies of 5, 10, and 20 kHz. Current values were inferred from the voltage generated across a small (710 Ω) resistor in series with the array. The lower set of (vertical) arrows in the figure indicates the voltage (240 ± 5 V_{rms}) at which the first device in the array ignites for each excitation frequency. The higher voltages denoted by the upper set of (horizontal) arrows in Fig. 5 represent the “all on” voltage

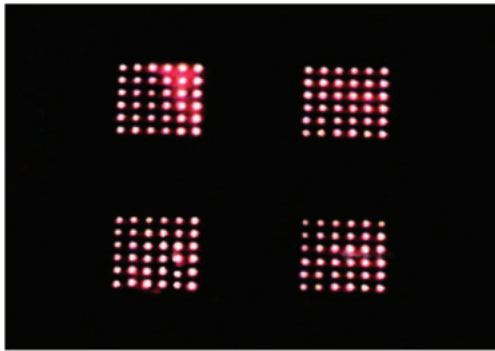


Fig. 4. Optical micrograph of four 6×6 arrays of $100\mu\text{m}$ dia. micro-cavity plasma devices operating in 500Torr of Ne. These Ni screen/ $30\mu\text{m}$ polyimide/ $3\mu\text{m}$ Cu devices are driven by a 20kHz sinusoidal voltage of $265\text{ V}_{\text{rms}}$.

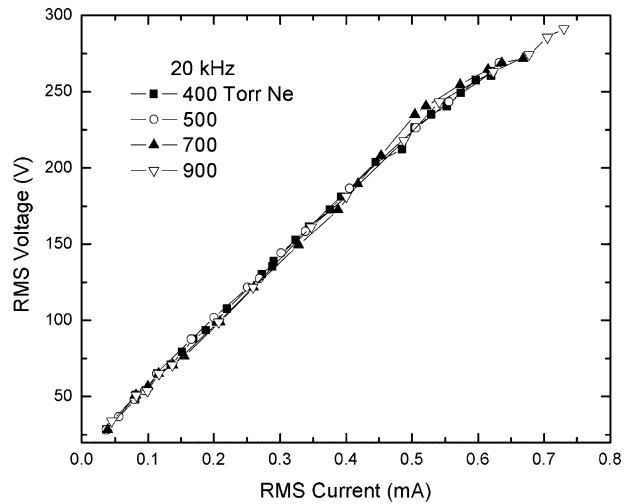


Fig. 6. Data similar to those of Fig. 5 but for the driving frequency fixed at 20kHz and the Ne pressure varied from 400 to 900 Torr.

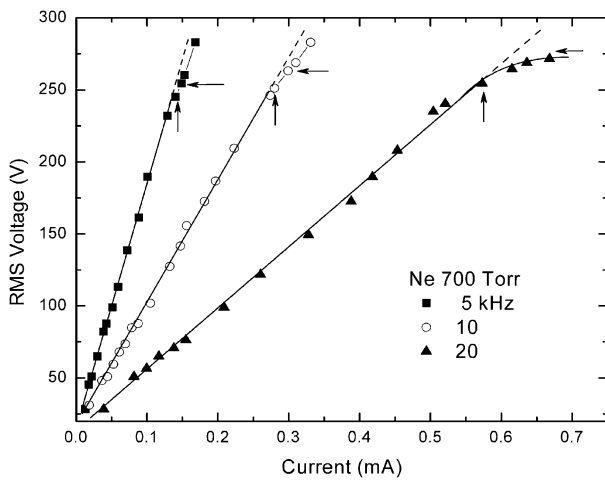


Fig. 5. V - I characteristics for the array of Fig. 4 for $p_{\text{Ne}} = 700\text{ Torr}$ and sinusoidal voltage frequencies of 5, 10, and 20kHz.

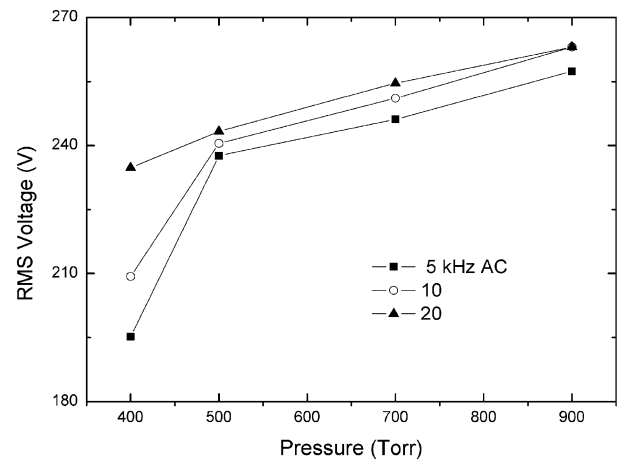


Fig. 7. Ignition voltages for the arrays of Figs. 5 and 6 and $p_{\text{Ne}} = 400$ – 900 Torr .

which is measured to be $265 \pm 10\text{ V}_{\text{rms}}$. For driving voltages below the ignition value, the array exhibits a large capacitive impedance [$\sim 1\text{ M}\Omega$ at 10kHz or $C_{\text{array}} = (17 \pm 1)\text{ pF}$] which is to be expected in view of the metal film/polymer/metal layered structure into which the microcavities are fabricated. Patterning the electrodes will undoubtedly lower the array capacitance considerably. Notice that the impedance of the array changes almost imperceptibly above ignition for the 5 kHz data whereas, at a driving frequency of 20kHz, a rapid decline in the overall impedance (device structure plus plasma) is evident above the array ignition voltage as the current is increased. Although the V - I characteristics have, to date, been examined over a small range in current ($<1\text{ mA}$), it is clear that once the contribution of displacement current to the total has been removed, the microplasmas at this pressure operate in the abnormal glow mode. Data similar to those of Fig. 5 but for which the driving voltage frequency was fixed at 20kHz are shown in Fig. 6 for Ne pressures between 400 and 900 Torr. The operating voltages exhibited by these devices are virtually independent of p_{Ne} but drawing further conclusions must await the availability of measurements at higher average currents. As illustrated in Fig. 7, however, the ignition voltages for the arrays reveal a significant (15–20%) rise between $p_{\text{Ne}} = 400$ and 500 Torr ($pd = 4$ – 5

Torr cm) when the sinusoidal driving frequency is 5 or 10kHz. The origin of this increase is not clear but may be attributed to several factors, one of which is the transition of the plasma from operating as a negative glow at lower pressures to the Townsend mode.^{9,10} A secondary contributor to this behavior appears to be associated with moving from Paschen's minimum at $\lesssim 4\text{ Torr cm}$ to higher pd values.

3.2 Performance of intentionally-damaged arrays

A decided asset of any microplasma device structure under consideration for commercial production is the potential robustness of the design—its tolerance to deviations from optimal manufacturing and operating conditions. In that vein, series of experiments have been performed in which arrays of devices having the structure of Fig. 1 were damaged *intentionally*. Part (a) of Fig. 8 is an optical micrograph of a subarray comprising microplasma devices with $100\mu\text{m}$ diameter cylindrical cavities. Each device is again overcoated with a $1.5\mu\text{m}$ thick film of silicon nitride and is fabricated in a Ni/ $30\mu\text{m}$ polyimide/ $3\mu\text{m}$ Cu layered substrate. In order to explore the performance of devices having microcavities with cross-sectional geometries other than circular, a second mask was placed in the optical train

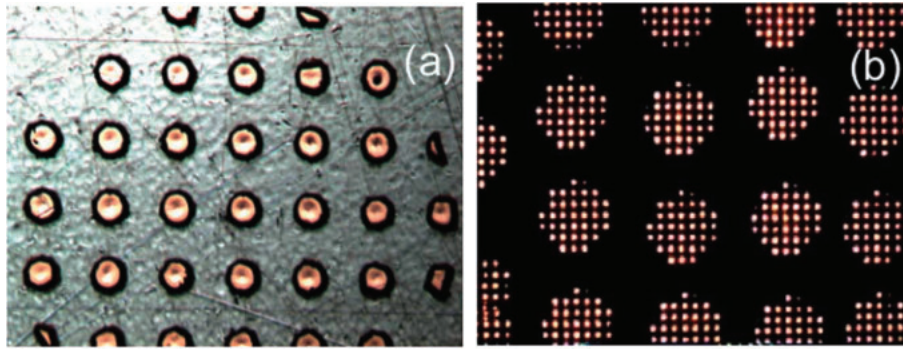


Fig. 8. Photographs illustrating the condition and operation of intentionally-damaged microcavity plasma arrays: (a) Optical micrograph of a segment of an array of Ni/30 μm polyimide/3 μm Cu devices that was damaged with an abrasive. Melting of the underlying Cu film is also evident; (b) Image, obtained with a telescope and CCD camera, of a segment of a large array comprising subarrays of ~ 35 individual devices, and operating in 500 Torr of Ne at an RMS voltage of 110 V. Note the two intentionally-overlapped subarrays at extreme lower left of the photograph.

of the photoablation system, adjacent to the mask responsible for the array pattern of Fig. 4. The result is that subarrays are produced in which most devices have the same microcavity size and pitch (200 μm) as those presented earlier, but the circular aperture serves to define the perimeter of the array and, in so doing, produces several devices with unusual shapes. As illustrated in Fig. 8(a), the insertion of the aperture yields devices with crescent-shaped, trapezoidal and even triangular cross-sections. It is also clear from Fig. 8(a) that the ablation process was modified so as to produce microcavities of poor quality, with irregular and spatially-varying cross-sections. Furthermore, the black ring at the outer edge of each device is the result of nonuniform ablation of the polyimide which is a direct result of the incident laser intensity profile. Finally, it was noted earlier that the entire device fabrication process was initially designed such that ablation ceased once the polyimide/Cu interface was reached. In the case of Fig. 8(a), however, the metal substrate was also irradiated which resulted in clear evidences of melting of the Cu film and, in several devices, the film was breached entirely.

If these steps were insufficient to sorely test the robustness of the device structure reported here, these arrays were additionally damaged by an abrasive. The scratching and gouging of the Ni surface brought about by mechanically abrading the surface are clearly seen in the photograph on the left side of Fig. 8.

Given this level of intentional damage to the arrays, it is remarkable that experiments demonstrate the reliable and stable operation of these devices. Figure 8(b) is an image, obtained with an optical telescope and a charge-coupled device (CCD) camera, of a segment of a large microplasma array comprising subarrays identical to that of Fig. 8(a) and operating in 500 Torr of Ne. No effort was made in the fabrication process to equally space the subarrays. On the contrary, at the extreme lower left of Fig. 8(b), two subarrays that were overlapped can be seen. Notice, too, the 2–4 small emitters that are present in every subarray in Fig. 8(b). These are the “truncated” devices having variable cross-sections that were discussed earlier [several are noticeable in Fig. 8(a)]. The point to be made is that virtually every device in the subarrays ignites, irrespective of the cross-sectional shape of its microcavity, and a high level

of emission uniformity is maintained across the overall array (constant to within $\pm 15\%$), despite the steps taken to impact adversely the array.

4. Conclusions

The operation of microcavity plasma devices fabricated in 3–5 μm Cu/ $\sim 30\mu\text{m}$ polyimide substrates has been described. Having a silicon nitride dielectric barrier film and microcavities produced by KrF laser ablation, these devices have been examined for Ne pressures between 400 and 900 Torr and are observed to be exceptionally robust and insensitive to variations in the microcavity cross-section. Despite intentional damage to the devices and fabrication parameters far from optimal values, virtually all microcavities in the array ignite despite the variety in cross-sectional shapes of the microcavities. These results bode well for efforts to develop microplasma arrays of large surface area, fabricated by large volume techniques such as roll-to-roll processing.

Acknowledgements

The assistance of D. Wright (Anvik) and K. Collier (Illinois), as well as the support of this work by the U.S. Air Force Office of Scientific Research under grant F49620-03-1-0391 and the National Science Foundation under the auspices of the Nano-CEMMS Center at the University of Illinois under grant NSF DMI 03-28162, is gratefully acknowledged.

- 1) A. D. White: *J. Appl. Phys.* **30** (1959) 711.
- 2) A. Koutsospyros, S.-Y. Yin, C. Christodoulatos and K. Becker: *Int. J. Mass Spectrom.* **233** (2004) 305.
- 3) A. Koutsospyros, S.-Y. Yin, C. Christodoulatos and K. Becker: *IEEE Trans. Plasma Sci.* **33** (2005) 42.
- 4) A. El-Habachi and K. H. Schoenbach: *Appl. Phys. Lett.* **73** (1998) 885.
- 5) K. H. Becker, K. H. Schoenbach and J. G. Eden: *J. Phys. D* **38** (2005) R55.
- 6) S.-J. Park, J. Chen, C. Liu and J. G. Eden: *Electron. Lett.* **37** (2001) 171.
- 7) S.-J. Park, C. J. Wagner, C. M. Herring and J. G. Eden: *Appl. Phys. Lett.* **77** (2000) 199.
- 8) R. M. Sankaran and K. P. Giapis: *Appl. Phys. Lett.* **79** (2001) 593.
- 9) M. J. Kushner: *J. Phys. D* **38** (2005) 1633.
- 10) M. J. Kushner: *J. Appl. Phys.* **95** (2004) 846.